JACS
JOURNAL OF THE AMERICAN CHEMICAL SOCIETY
Article
pubs.acs.org/JACS

# Electric Field Breakdown in Single Molecule Junctions

Haixing Li,[†] Timothy A. Su,[‡] Vivian Zhang,[‡] Michael L. Steigerwald,*[,‡] Colin Nuckolls,*[,‡] and Latha Venkataraman*[,†]

[†]Department of Applied Physics and Applied Mathematics and [‡]Department of Chemistry, Columbia University, New York, New York 10027, United States

Supporting Information

**ABSTRACT:** Here we study the stability and rupture of molecular junctions under high voltage bias at the single molecule/single bond level using the scanning tunneling microscope-based break-junction technique. We synthesize carbon-, silicon-, and germanium-based molecular wires terminated by aurophilic linker groups and study how the molecular backbone and linker group affect the probability of voltage-induced junction rupture. First, we find that junctions formed with covalent S−Au bonds are robust under high voltage and their rupture does not demonstrate bias dependence within our bias range. In contrast, junctions formed through donor−acceptor bonds rupture more frequently, and their rupture probability demonstrates a strong bias dependence. Moreover, we find that the junction rupture probability increases significantly above ∼1 V in junctions formed from methylthiol-terminated disilanes and digermanes, indicating a voltage-induced rupture of individual Si−Si and Ge−Ge bonds. Finally, we compare the rupture probabilities of the thiol-terminated silane derivatives containing Si−Si, Si−C, and Si−O bonds and find that Si−C backbones have higher probabilities of sustaining the highest voltage. These results establish a new method for studying electric field breakdown phenomena at the single molecule level.

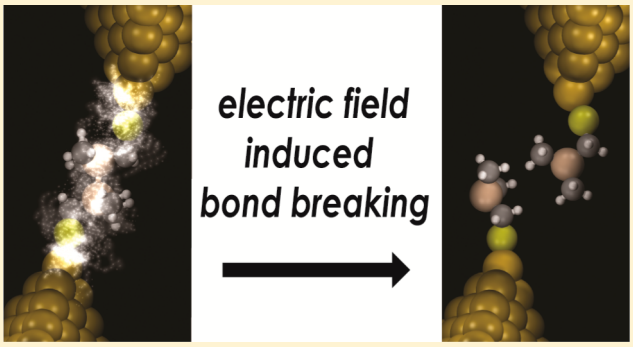


## INTRODUCTION

A challenge in the semiconductor industry is to lower the dielectric constant ($\kappa$) of the dielectric material without diminishing its ability to withstand breakdown in strong electric fields. Low-$\kappa$ materials have a lower dielectric constant than traditional $SiO_2$ dielectric materials and therefore improve device speed as well as power efficiency. However, low-$\kappa$ materials are less robust than traditional dielectric materials and degrade through a mechanism referred to as time dependent dielectric breakdown.[1] While many theoretical models[2] have been developed to rationalize electric field breakdown in silicon-based networks[3] of three-dimensional (3D) low-$\kappa$ materials, an experimental study of voltage-induced breakdown at the single bond level is lacking.[4]

Here we report the voltage-induced breakdown characteristics of single bonds commonly found in semiconductor materials. We study the behavior of these bonds in the context of a single molecule junction with the scanning tunneling microscope-based break-junction technique (STM-BJ). We alter the structure of the molecular backbone to include either Si−Si, Ge−Ge, C−C, Si−C, or Si−O bonds and study the effect of a high electric field on each of these individual bonds. This enables us to determine how each atomic component contributes to the field-induced bond rupture. We show that (1) junction rupture probability increases with applied voltage for Au-linker donor−acceptor bonds but remains constant with increasing voltage for covalent Au−S bonds; (2) molecular junctions containing a single Si−Si or Ge−Ge bond have an abrupt increase in rupture probability above 1 V, indicating Si−Si/Ge−Ge bond rupture; (3) molecular junctions with Si−Si and Si−O bonds demonstrate a higher rupture probability relative to those with only Si−C bond at voltages exceeding 1 V; and (4) the rupture probability for junctions formed with covalent Au−S bonds is positively correlated with the molecular junction conductance; such a correlation is not seen for donor−acceptor bonded junctions. Our results from this study of electric field breakdown at the single molecule level provide guidance for designing low-$\kappa$ dielectric materials as well as molecular devices that require stability under high voltage bias.

## RESULTS AND DISCUSSION

**Experimental Method.** We use the STM-BJ technique[5] to determine the stability and rupture probability of single molecule junctions under an applied voltage (Figure 1a) as detailed in the Methods section. Unlike the standard STM-BJ measurements where Au point contacts are pulled apart in a solution of molecules while measuring conductance, here we develop a new technique to evaluate the breakdown voltage of single molecule junctions that contain different chemical bonds.

Received: December 9, 2014

 © XXXX American Chemical Society 

DOI: 10.1021/ja512523r
J. Am. Chem. Soc. XXXX, XXX, XXX−XXX

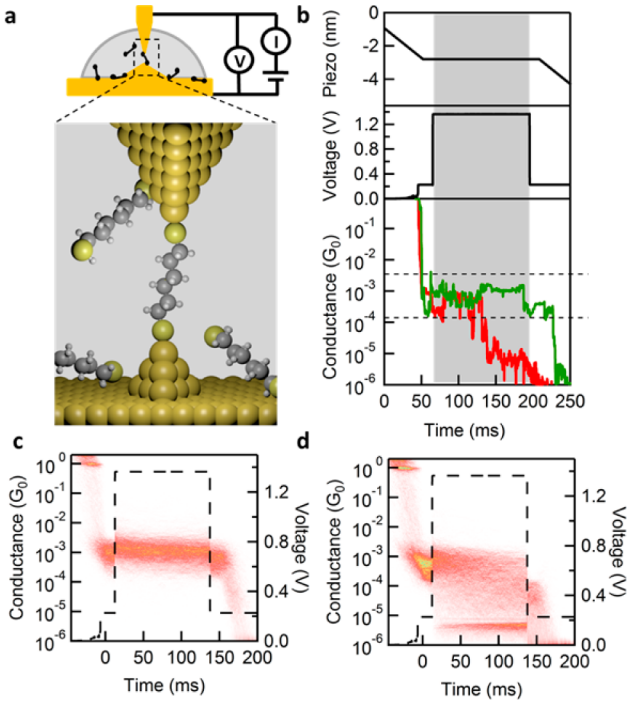


**Figure 1.** (a) Schematic of experimental setup and cartoon of a single molecule junction formed with 1,6-hexanedithiol. (b) Upper panel: piezo displacement versus time. Middle panel: applied voltage versus time. Lower panel: two sample traces measured with the molecule 1,6-hexanedithiol. The green (red) curve represents a molecular junction that sustains (ruptures) under the bias. Note the bias across the junction is very low before 1 $G_0$ rupture due to a 100 kΩ resistor placed in series with the junction. Two-dimensional histograms made from traces with 1,6-hexanedithiol that sustain (c) and rupture (d) while applying a bias voltage as shown by the dashed line. The flat feature below $10^{-5}$ $G_0$ in (d) is from measurements of broken junctions at 1.4 V.

We modify the ramp applied to the STM piezoelectric transducer to hold the junction in place for 150 ms during each measurement and apply a voltage pulse ranging in amplitude from 0.2 to 1.4 V (gray-colored areas in Figure 1b) during this "hold" section.[6] In Figure 1b we show example traces measured for 1,6-hexanedithiol junction that either sustains the voltage pulse for the entire hold period (green) or breaks during the hold (red).

We analyze all data using an automated algorithm (see Methods section for details) to statistically determine the percentage of junctions that break during their measurement. We determine the conductance of the trace prior to the voltage pulse to ensure that we are selecting a trace where a molecule is bridging the electrodes. We then use the conductance after the pulse to sort the junctions into two types: those that persist and those that break under the bias. We create 2D overlays of all traces that either sustain or break and align them to the start of the "hold". Figure 1c,d shows such 2D histograms from data obtained while applying a 1.4 V bias to Au-1,6-hexanedithiol-Au junctions. In Figure 1c, the histogram of traces that do not break shows that the conductance remains roughly constant throughout the hold section, indicating that we are indeed maintaining a molecular junction. We also see a slight increase in conductance when we apply the 1.4 V voltage pulse, which is seen in most of the molecules we tested here (see Supporting Information (SI) Figures S5–S17). This shows that the bias window used here goes beyond the linear current–voltage regime for most molecules.[7] The histogram in Figure 1d demonstrates that junctions tend to break shortly after the high bias is applied. As we will show later in the manuscript, the break time distribution follows an exponential decay. We note that molecular backbones that are terminated by thiols at each end ("dithiol junctions") have a broader distribution of conductance values compared to molecular backbones terminated with the dative linkers in this study.[8] However, for the measurements discussed here, we do not distinguish different types of dithiol junctions based on conductance values. We simply analyze all junction and contact conformations together.

**Varying Linker.** We first apply our measurement technique to investigate the impact of different electrode linker groups on the stability of the molecular junction under applied electric field. For this study, we measure a series of $\alpha,\omega$-difunctionalized hexane backbones with thiol, amine,[5b] methylsulfide,[9] and diphenylphosphine[10] terminations. Specifically, we compare rupture probabilities in junctions formed with 1,6-hexanedithiol (**1**), 1,6-hexanediamine (**2**), 1,6-bis(thiomethyl)hexane (**3**), and 1,6-bis(diphenylphosphino)-hexane (**4**) as illustrated in Figure 2a. We employ the method outlined above to determine

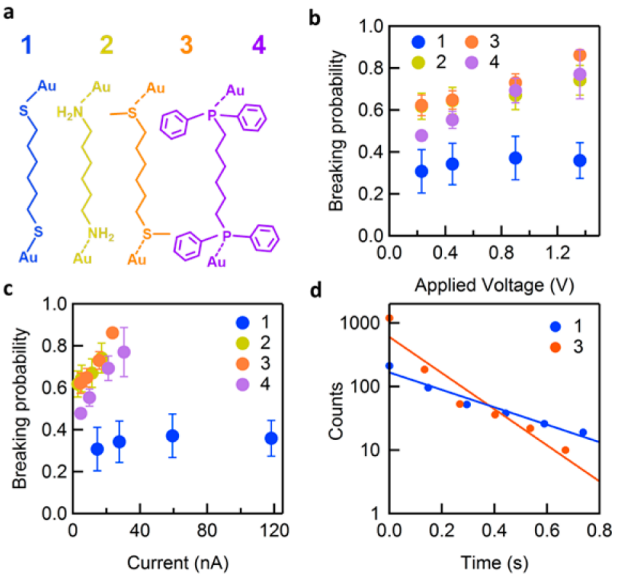


**Figure 2.** (a) Structures of molecules **1**–**4**. Junction breaking probability plotted against (b) applied bias voltage and (c) current through the junction for **1**–**4**. The error bars show the standard deviation determined from variations in sets of thousand measurements. (d) Histograms of junction rupture time made from 500 measurements of **1** (blue dots) and 1500 measurements of **3** (orange dots). The linear fits on a semilog scale (blue and orange lines) indicate an exponential decay with decay time $\tau$ = 0.32 s for **1** and $\tau$ = 0.15 s for **3**.

the rupture probability for each molecule at different bias voltages. In Figure 2b, we plot the junction rupture probability as a function of applied voltage. Junctions formed with **1** have the lowest rupture probability, and the probability of rupture is independent of the magnitude the applied voltage (up to $V$ = 1.4 V). The rupture probability is much higher for **2**–**4** compared to **1**; the rupture probabilities for **2**–**4** also increase with increasing bias voltage. Figure 2c shows the rupture probability as a function of the current flowing through the


DOI: 10.1021/ja512523r
J. Am. Chem. Soc. XXXX, XXX, XXX–XXX

junction and depicts a similar trend: **2**–**4** show a linear increase in rupture probability as the current through the junction increases, while the rupture probability of **1** remains constant as current increases. We attribute this difference to the nature of bonding between the molecule and gold electrode. Molecules **2**–**4** form donor–acceptor bonds[9,10] between the N (**2**), S (**3**), and P (**4**) lone pairs and the undercoordinated gold atoms on the electrode surface. These bonds are inherently weak with a binding energy ranging from 0.5 to 1.2 eV.[9,10] In contrast, **1** forms a covalent Au–S[11] bond with a binding energy around 2 eV[12] that enables thiols to form robust junctions that withstand a high applied voltage.

Our measurements show that the covalently linked systems have a voltage-independent rupture probability across the whole bias range that we apply, while the donor–acceptor linked systems have a voltage-independent rupture probability below ~0.2 V (see SI Figure S1) and a strong voltage dependence above ~0.2 V. We explain the results of both systems as follows. The voltage independent rupture that is seen most clearly for **1** at all voltages and for **2**–**4** at low voltages is attributed to thermally activated processes due to room temperature measurement or mechanically induced rupture due to vibrations inherent to our STM setup. Indeed, if we add a white noise modulation with a 1 Å amplitude to the piezo (SI Figure S2a), we see an increase in junction rupture probability irrespective of the voltage applied (SI Figure S2b). In contrast, the junction rupture that occurs in donor–acceptor linked junctions with increasing voltage arises from a voltage-activated process. We hypothesize that this voltage-induced rupture results from electrons exciting vibrational modes of the linker-gold bonds. Previous inelastic electron tunneling spectroscopy (IETS) studies have shown that the voltage required to excite a Au–S stretching mode in a mechanically controlled break-junction (MCBJ) measurement of 1,8-octanedithiol between Au electrodes is 35 mV, while the voltage to excite the Au–N stretching mode for the donor–acceptor linked junction with 1,8-octanediamine is 29 mV.[13] When the applied voltage exceeds the IETS threshold, the incoming electrons are able to excite the vibrational mode, which can in turn lead to bond rupture, though the probability for rupture will also depend on the bond energy. The higher the applied voltage, the higher the current through the junction and hence a higher probability of exciting a vibrational mode. The fact that a voltage-dependent rupture is not seen in **1** is likely due to its higher binding energy. Rupture of the Au–S bond would require multiple excitations to occur, requiring a higher current and consequently a higher voltage range than what we apply in these experiments.

Additionally, the presence of an electric field can polarize and weaken a bond. Calculations show that the voltage drop across a Au–S[14] covalent bond is much smaller than that across a Au-SMe donor–acceptor bond,[15] suggesting that the donor–acceptor interactions experience strong voltage-induced bond weakening. Additionally, we note that the voltage drop across the Au electrode and the Au–Au bonds within the junction is considerably smaller than that across the Au-linker bond or the molecular backbone.[14] Taken together, we can conclude that the voltage applied across the molecular junction can polarize and weaken the Au-linker bond; if it is larger than the threshold voltage for exciting bond vibrational modes, it can control bond rupture by determining the junction current.

Next, we compare the length of time that each junction can sustain an applied voltage 1.4 V before it ruptures. For these measurements, we modify the ramp applied to the piezoelectric transducer to hold the junction at a fixed displacement for 1.5 s. We only consider traces with a molecular junction at the start of the hold and determine the time that the junction ruptures within the hold section. We use the automated algorithms detailed in the Methods section for all analyses. We generate a histogram of the break times, as shown in Figure 2d for **1** and **3**. We fit each distribution with an exponential function $P = P_0 e^{-t/\tau}$ (lines in Figure 2d) and find that molecule **1** has decay time constant $\tau = 0.32$ s, twice that of molecule **3** ($\tau = 0.15$ s). This result confirms that single molecule junctions formed with Au–S covalent bonds are less likely to rupture under an applied voltage and can sustain the bias for longer time when compared with the molecular junctions formed with donor–acceptor bonds.

**Varying Backbone.** Our study of the rupture behavior of different linker groups under applied voltage suggests that methylthiol ($-CH_2SH$) linkers provide a promising test bed to study how different molecular analogs of low-$\kappa$ dielectric materials influence junction breakdown under an applied voltage. We synthesized all silanes and germanes following the method showing in Scheme 1 and detailed in the Methods section.

**Scheme 1. General Approach for Installing Methylthiol Linkers on the Silanes and Germanes**[a]

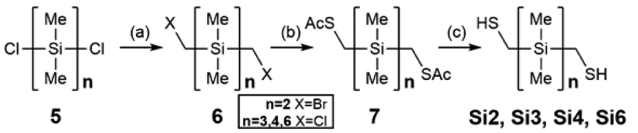


[a](a) For $n = 2$: LiBr, $CH_2Br_2$, *n*-BuLi, THF, −78°C. For $n$ = 3,4,6: $CH_2BrCl$, *n*-BuLi, THF, −78°C; 69–93% yield. (b) KSAc, THF, reflux; 37–75% yield. (c) $LiAlH_4$, $Et_2O$, 0°C; 51–84% yield.

We measured the conductance of the oligosilanes using our standard STM-BJ method. Figure 3a shows the normalized log-binned conductance histograms constructed from approximately 30,000 measured traces for each molecule without any data selection. We obtained an average conductance for these junctions by fitting the conductance peak with a Gaussian function. In Figure 3b, we plot the conductance peak value as a function of the number of silicon atoms in the backbone on a semilog scale. We find that the conductance decays

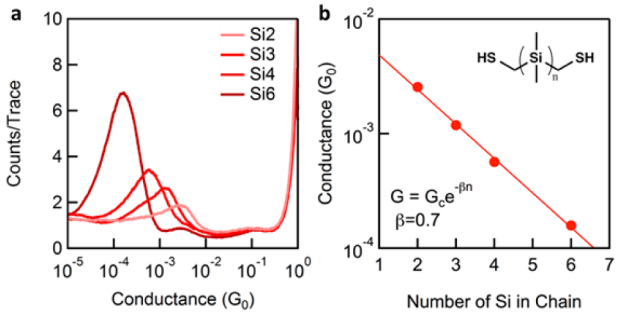


**Figure 3.** (a) Logarithm-binned 1D conductance histograms of molecules **Si2**–**4** and **Si6** (100 bins/decade). (b) Conductance peak values are plotted against the number of silicon atoms in the backbone of molecules **Si2**–**4** and **Si6**. The decay constant ($\beta$) for the permethyloligosilanes with $CH_2SH$ linkers is 0.70 ± 0.02 per Si atom.


DOI: 10.1021/ja512523r
J. Am. Chem. Soc. XXXX, XXX, XXX–XXX

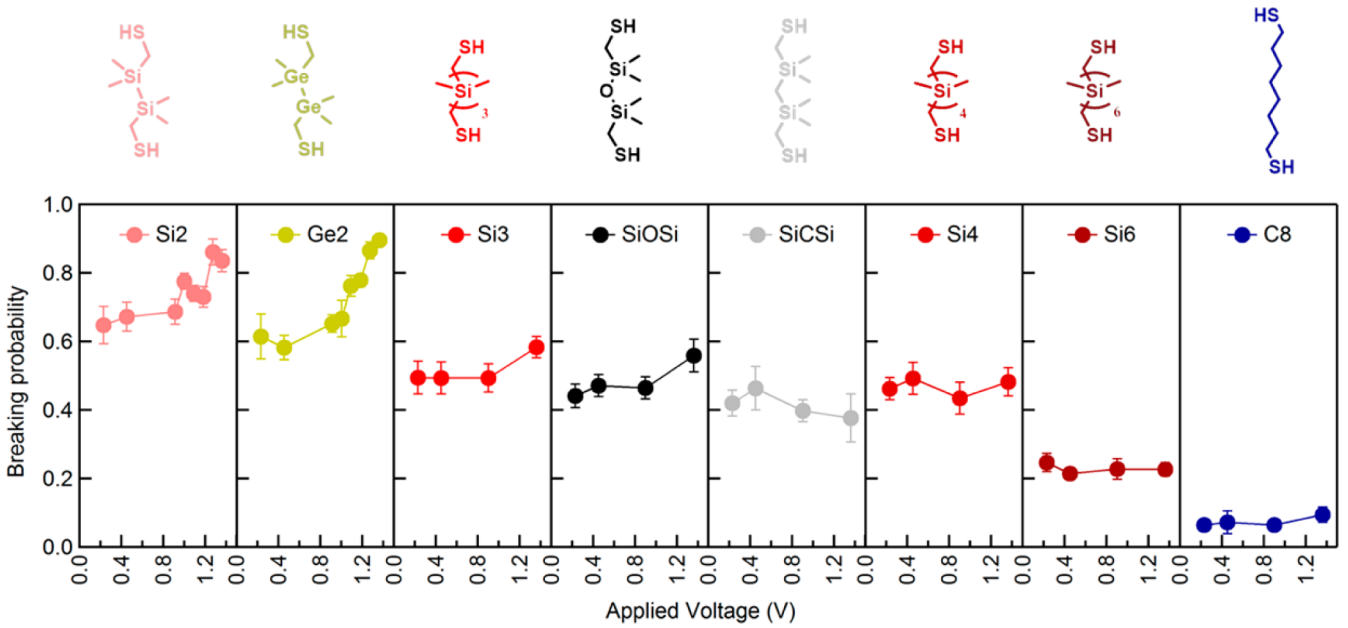


**Figure 4.** Junction rupture probability plotted against the applied voltage for $CH_2SH$-terminated molecules. The molecular structures are shown above their respective measurement data. Error bars show the standard deviation determined from variations in sets of thousand measurements.

exponentially with $n$, the number of Si atoms in the chain, as $G \sim e^{-\beta n}$. The tunneling decay constant $\beta$ is 0.70 ± 0.02 per Si atom, determined by fitting a line using the least-squares method. Here we will use this $CH_2$−SH terminated series for the bias-dependent rupture measurements.

We carry out junction rupture measurements at voltages ranging from 0.2 to 1.4 V for the oligosilanes and compare these results with alkanes, germanes, and other silane derivatives. We use the same general technique outlined in Scheme 1 to synthesize **Ge2**, **SiOSi**, and **SiCSi** (Figure 4). In Figure 4, we plot the fraction of junctions that rupture as a function of the applied bias voltage. **Si2** and **Ge2** show a roughly constant rupture probability below 1 V and a roughly linear increase in rupture probability with voltage above 1 V. This constant rupture probability below 1 V is attributed to the thermally or mechanically activated rupture mechanisms described above. The increase in rupture probability observed for the **Si2** and **Ge2** above 1 V is distinct from the constant rupture probability we observe for the **C6** (Figure 2b) and **C8** (Figure 4) alkane analogs: this suggests that a bond other than the Au−S or Au−Au[16] bond is breaking. Our experimental data suggest that we are breaking the Si−Si and Ge−Ge bonds in these systems. This interpretation is supported by the well-established trends in bond strength and atomic polarizability in Group 14 elements as they descend the periodic table. The bond strengths for C−C, Si−Si, and Ge−Ge bonds are 3.7, 2.3, and 1.9 eV respectively, which implies that C−C bonds are significantly harder to break.[17] Polarizability describes the ease with which an electron cloud can be distorted in response to an external electric field. This suggests that large, "soft" bonds can be influenced to break more easily under a high voltage bias than small, "hard" bonds.

The polarizability calculated for C atoms is 1.67 au, while Si and Ge atomic polarizabilities are 5.53 and 5.84 au, respectively.[18] These trends are consistent with our measurement results which indicate that junctions formed with the germanes and silanes are more likely to rupture under a high bias than those formed with the alkanes.

Figure 4 also depicts a comparison of rupture probabilities in $-SiMe_2-X-SiMe_2-$ molecular backbones where X = $SiMe_2$, $CH_2$, or O. We find that junctions formed with **$Si_3$** and **SiOSi** show a slight increased rupture probability above 1 V, but **SiCSi** does not (Figure 4). This suggests that the Si−C−Si bond array has a higher capacity for sustaining large applied voltages compared to Si−O−Si and Si−Si−Si arrays. The latter two differ from the former in two distinct ways: the Si−O bonds are more polar than the Si−C bonds, and the Si−Si bonds are more polarizable than the Si−C bonds. These features could explain our results, although detailed calculations would be required to understand the impact of an applied bias on these systems. The more polar Si(+)−O(−)−Si(+) molecule should couple more strongly to the applied field, perhaps even leading to the heterolytic cleavage of one of the Si−O bonds. In a similar way, although the Si−Si−Si structure itself is nonpolar, in the presence of the applied field the Si−Si bonds, being more polarizable, should also couple more strongly to the applied field.

Results shown in Figure 4 indicate that we do not see voltage-dependent rupture in the longer silanes (**Si4** and **Si6**). This can be explained by considering the mechanism for voltage-induced bond rupture detailed above. In these longer silanes, the field across each bond is smaller, and thus the bonds are less polarized. Additionally, the current through these junctions is smaller and results in a reduced probability for exciting vibrational modes. Since there are more vibrational modes that can be excited in these longer systems, the probability of a single bond rupturing is lower.

We now look at the junction rupture probability as a function of molecular junction conductance. We use the 2D conductance−time histograms and integrate all counts, while the voltage pulse is applied to determine the average conductance value at the applied voltage (details shown in SI Figures S4−S17). In Figure 5a, we plot the rupture probabilities against these conductance values for all molecules shown in Figure 4 and for measurements of molecule **1** on a semilogarithm scale. For each molecule, the junction


DOI: 10.1021/ja512523r
J. Am. Chem. Soc. XXXX, XXX, XXX−XXX

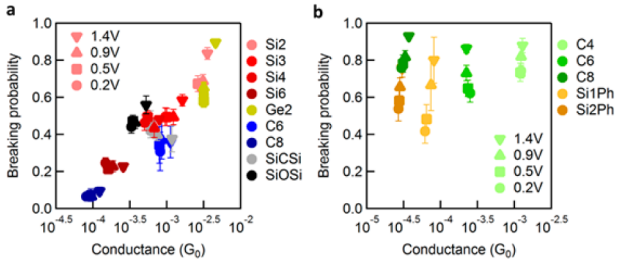


**Figure 5.** Junction rupture probability plotted against the conductance for (a) all thiol-terminated molecules from Figure 4 and **C6** (molecule **1** in Figure 2) and (b) for SMe-terminated molecules on a semilogarithm scale. The shape of the marker indicates the applied voltage: circle is 0.2 V, square is 0.5 V, up triangle is 0.9 V and down triangle is 1.4 V. Error bars show the standard deviation determined from variations in sets of thousand measurements.

conductance depends slightly on the applied bias voltage. However, the most striking result is that the rupture probability increases linearly with the logarithm of the conductance. In contrast, we do not see a dependence of the breaking probability on the heat produced (calculated as (current) × (voltage)) for each junction (as shown in SI Figure S18), which indicates that a local heating mechanism cannot explain the breaking process measured here. Finally, to compare this with results from junctions formed through donor–acceptor links, we show in Figure 5b analogous results from measurements of methylsulfide-terminated alkanes and silanes (structures shown in SI Figure S3). We see a clear increase in the rupture probability as the voltage increases. However, we find that there is no correlation between the rupture probability and molecular junction conductance for these methylsulfide-terminated junctions. These results provide a new perspective with which to distinguish donor–acceptor linked and covalent linked molecular junctions.

## CONCLUSIONS

In this report, we have used a modified STM-BJ technique to probe the rupture probability of single molecule junctions under applied voltage. We find that the junctions formed through donor–acceptor linkers have a lower threshold voltage for rupture than those formed with covalent linkers. Moreover, our results provide evidence that Si–Si and Ge–Ge bonds rupture above 1 V. Finally, we show that the Si–C bond is more robust under applied voltage than either the Si–Si or the Si–O bond. This study demonstrates that we can detect voltage-induced bond rupture in single molecule junctions. This provides a new approach to investigate the problem of time-dependent dielectric breakdown in low-$\kappa$ materials and also sheds light on the reliability of molecular electronic devices under applied voltage.

## METHODS

**Synthetic Details.** Molecules 1,6-hexanedithiol (**1**), 1,6-hexanediamine (**2**), 2,9-dithiadecane (**3**), and 1,6-bis(diphenylphosphino)-hexane (**4**) as illustrated in Figure 2a are obtained from Fluka (97%), Sigma-Aldrich (98%), Alfa Aesar (97%), and Sigma-Aldrich (97%), respectively, and used without further purification. We synthesized all silanes and germanes with methylthiol linkers by the same general method. We previously reported the synthesis of $\alpha,\omega$-dichlorooligosilanes.[19] Here, we react the $\alpha,\omega$-dichlorooligosilane **5** with a halomethyllithium species to furnish the $\alpha,\omega$-bis(halomethyl)-oligosilane **6** (Scheme 1).[20] We obtain the $\alpha,\omega$-bis(acetylthiomethyl)-oligosilane **7** by nucleophilic substitution of the primary halide with potassium thioacetate; we convert the resulting compounds to the final $\alpha,\omega$-bis(methylthiol)oligosilane **Si**$_n$ ($n$ = 2, 3, 4, 6) via lithium aluminum hydride reduction.[21] See SI for characterization and methods for synthesis of the molecules used here.

**Experimental Details.** STM-BJ experiments are carried out in a custom instrument designed to have a high mechanical stability under ambient conductions. The STM tip is a gold wire (0.25 mm diameter, Alfa Aesar, 99.999% purity), and the substrate is a thermally evaporated gold-on-mica substrate. Measurements are carried out at room temperature under ambient conditions in a ~1 mM solution of the target molecule in 1,2,4-tricholorobenzene (Alfa Aesar, 99%). For the standard STM-BJ experiment, we start by making a gold–gold contact with a conductance >5 $G_0$ ($G_0 = 2e^2/h$, quantum of conductance) and then withdraw the tip at a rate of 37 nm/s to break the junctions. We collect 30,000 traces and create logarithmically binned 1D histograms of these traces to determine the molecular junction conductance. For the rupture probability measurements, we modify this by first pulling a distance of 2.8 nm, holding the tip at a constant distance from the substrate for 150 ms (or 1.5 s), then pulling an additional 2.8 nm to break the junction. During the "hold", we apply a bias of 0.2, 0.5, 0.9, or 1.4 V for 125 ms to the junction. For molecules **Si2** and **Ge2**, we additionally collected data at 1, 1.1, 1.2, and 1.3 V. For each bias voltage, we collect 5000 traces.

**Data Analysis Details.** We first fit a Gaussian to the 1D conductance histogram peaks to obtain a conductance range for each molecule based on the peak position and width. We analyze the conductance during first and last 12.5 ms of the hold measurements to determine if the trace has a molecule bridging the gap between the electrodes. We require the average conductance of the 12.5 ms period before the voltage peak to be within the full-width of the conductance histogram peak. Among these selected traces, we determine the fraction that rupture under the bias by determining the conductance at the 12.5 ms period after the voltage peak. If this is within the full-width of the conductance histogram peak, then the junction did not rupture.

In order to know the break time for junctions that break within the hold, we apply an automated algorithm as illustrated in SI Scheme S1 that looks for the first large conductance drop during the hold. We require the average conductance before this drop to be within the full-width of the conductance histogram peak to ensure a molecular junction. The time at which this drop is observed is the junction breaking time. We compile these times determined from 500 to 1000 junctions to generate a histogram and perform a statistical study.

## ASSOCIATED CONTENT

### Supporting Information

Supplemental figures, synthetic procedures, and characterization of compounds. This material is available free of charge via the Internet at http://pubs.acs.org.

## AUTHOR INFORMATION

### Corresponding Authors

*mls2064@columbia.edu
*cn37@columbia.edu
*lv2117@columbia.edu

### Notes

The authors declare no competing financial interest.

## ACKNOWLEDGMENTS

H.L. is supported by the Semiconductor Research Corporation and New York CAIST program. T.A.S. is supported by the NSF Graduate Research Fellowship under grant no. 11-44155. We thank the NSF for the support of these studies under grant no. CHE-1404922.



DOI: 10.1021/ja512523r
J. Am. Chem. Soc. XXXX, XXX, XXX–XXX

## REFERENCES


(1) (a) Chen, F.; Shinosky, M. *IEEE Trans. Electron Devices* **2009**, *56*, 2. (b) Chen, F.; Bravo, O.; Harmon, D.; Shinosky, M.; Aitken, J. *Microelectronics Reliability* **2008**, *48*, 1375.

(2) (a) Chen, F.; Shinosky, M. A. *Microelectron. Reliab.* **2014**, *54*, 529. (b) Wu, E. Y.; Li, B.; Stathis, J. H. *Appl. Phys. Lett.* **2013**, *103*, 152907. (c) Lombardo, S.; Stathis, J. H.; Linder, B. P.; Pey, K. L.; Palumbo, F.; Tung, C. H. *J. Appl. Phys.* **2005**, *98*, 121301. (d) McPherson, J. W. *Microelectron. Reliab.* **2012**, *52*, 1753.

(3) (a) Maex, K.; Baklanov, M.; Shamiryan, D.; Brongersma, S.; Yanovitskaya, Z. *J. Appl. Phys.* **2003**, *93*, 8793. (b) Volksen, W.; Miller, R. D.; Dubois, G. *Chem. Rev.* **2010**, *110*, 56.

(4) (a) Patitsas, S. N.; Lopinski, G. P.; Hul'ko, O.; Moffatt, D. J.; Wolkow, R. A. *Surf. Sci.* **2000**, *457*, L425. (b) Foley, E.; Kam, A.; Lyding, J.; Avouris, P. *Phys. Rev. Lett.* **1998**, *80*, 1336. (c) Shen, T. C.; Wang, C.; Abeln, G. C.; Tucker, J. R.; Lyding, J. W.; Avouris, P.; Walkup, R. E. *Science* **1995**, *268*, 1590.

(5) (a) Xu, B. Q.; Tao, N. J. *Science* **2003**, *301*, 1221. (b) Venkataraman, L.; Klare, J. E.; Tam, I. W.; Nuckolls, C.; Hybertsen, M. S.; Steigerwald, M. L. *Nano Lett.* **2006**, *6*, 458.

(6) Reichert, J.; Ochs, R.; Beckmann, D.; Weber, H. B.; Mayor, M.; Löhneysen, H. v. *Phys. Rev. Lett.* **2002**, *88*, 176804.

(7) Darancet, P.; Widawsky, J. R.; Choi, H. J.; Venkataraman, L.; Neaton, J. B. *Nano Lett.* **2012**, *12*, 6250.

(8) Venkataraman, L.; Klare, J. E.; Tam, I. W.; Nuckolls, C.; Hybertsen, M. S.; Steigerwald, M. L. *Nano Lett.* **2006**, *6*, 458.

(9) Park, Y. S.; Whalley, A. C.; Kamenetska, M.; Steigerwald, M. L.; Hybertsen, M. S.; Nuckolls, C.; Venkataraman, L. *J. Am. Chem. Soc.* **2007**, *129*, 15768.

(10) Parameswaran, R.; Widawsky, J. R.; Vazquez, H.; Park, Y. S.; Boardman, B. M.; Nuckolls, C.; Steigerwald, M. L.; Hybertsen, M. S.; Venkataraman, L. *J. Phys. Chem. Lett.* **2010**, *1*, 2114.

(11) Bain, C. D.; Troughton, E. B.; Tao, Y. T.; Evall, J.; Whitesides, G. M.; Nuzzo, R. G. *J. Am. Chem. Soc.* **1989**, *111*, 321.

(12) Ulman, A. *Chem. Rev.* **1996**, *96*, 1533.

(13) Kim, Y.; Hellmuth, T. J.; Bürkle, M.; Pauly, F.; Scheer, E. *ACS Nano* **2011**, *5*, 4104.

(14) Taylor, J.; Brandbyge, M.; Stokbro, K. *Phys. Rev. Lett.* **2002**, *89*, 138301.

(15) Batra, A.; Darancet, P. T.; Chen, Q.; Meisner, J.; Widawsky, J. R.; Neaton, J. B.; Nuckolls, C.; Venkataraman, L. *Nano Lett.* **2013**, *13*, 6233.

(16) (a) Frei, M.; Aradhya, S. V.; Hybertsen, M. S.; Venkataraman, L. *J. Am. Chem. Soc.* **2012**, *134*, 4003. (b) Huang, Z. F.; Chen, F.; Bennett, P. A.; Tao, N. J. *J. Am. Chem. Soc.* **2007**, *129*, 13225.

(17) Sanderson, R. T. *J. Am. Chem. Soc.* **1983**, *105*, 2259.

(18) Thierfelder, C.; Assadollahzadeh, B.; Schwerdtfeger, P.; Schäfer, S.; Schäfer, R. *Phys. Rev. A* **2008**, *78*, 52506.

(19) Klausen, R. S.; Widawsky, J. R.; Steigerwald, M. L.; Venkataraman, L.; Nuckolls, C. *J. Am. Chem. Soc.* **2012**, *134*, 4541.

(20) (a) Kobayashi, T.; Pannell, K. H. *Organometallics* **1990**, *9*, 2201. (b) Kobayashi, T.; Pannell, K. H. *Organometallics* **1991**, *10*, 1960.

(21) (a) Block, E.; Dikarev, E. V.; Glass, R. S.; Jin, J.; Li, B.; Li, X.; Zhang, S.-Z. *J. Am. Chem. Soc.* **2006**, *128*, 14949. (b) Apfel, U. P.; Troegel, D.; Halpin, Y.; Tschierlei, S.; Uhlemann, U.; Gorls, H.; Schmitt, M.; Popp, J.; Dunne, P.; Venkatesan, M.; Coey, M.; Rudolph, M.; Vos, J. G.; Tacke, R.; Weigand, W. *Inorg. Chem.* **2010**, *49*, 10117.




DOI: 10.1021/ja512523r
*J. Am. Chem. Soc.* XXXX, XXX, XXX−XXX